Supporting Information

Study on the preparation of ascorbic acid reduced ultrafine copper powders in the presence of different protectants and the properties of copper powders based on methionine protection

Xin Ke, [a,b,c] *Bingqing Xie,* [a,b,c] *Jingguo Zhang,** [a,b,d] *Jianwei Wang,** [a,e] *Weiying Li,* [b] *Liqing Ban,* [a,b] *Qiang Hu,* [a,b] *Huijun He,* [a,b] *Limin Wang,* [a,b] *Zhong Wang** [a,b]

[a] *Metal Powder Materials Industrial Technology Research Institute of CHINA GRINM, Beijing 101407, China*

[b] *GRIPM Advanced Materials Co. Ltd., Beijing 101407,*

[c] *General Research Institute for Nonferrous Metals, Beijing 100088, China*

[d] *China Gricy Advanced Materials Co., Ltd., Chongqing 401431, China*

[e] *GRINM NEXUSX Advanced Materials (Beijing) Co. Ltd., Beijing 101407, China*

Zhong Wang, *Corresponding author: wzwz99@126.com.

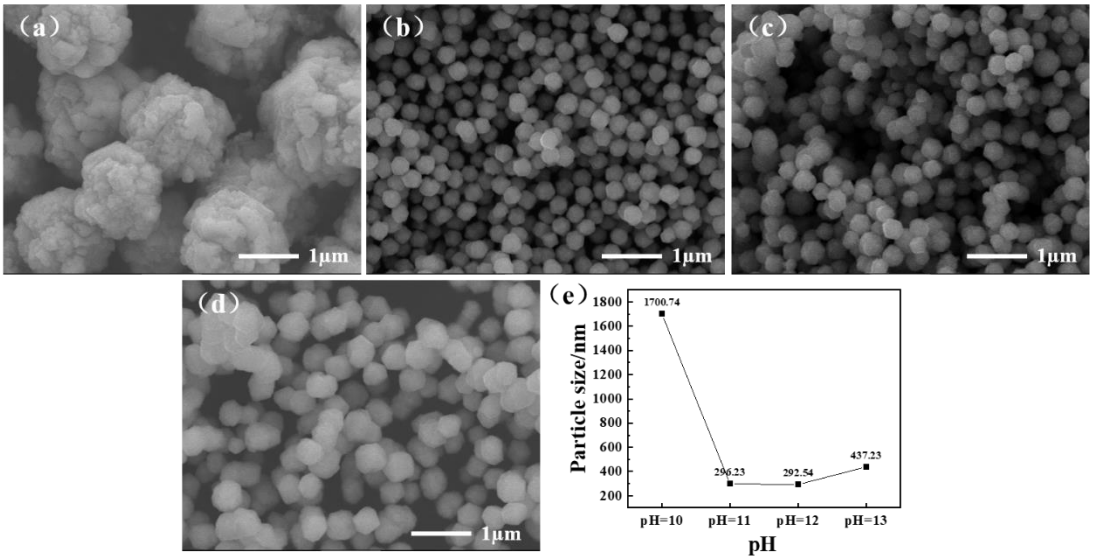

Fig. S1. SEM images and particle size variation of copper powder particles under different pH conditions using Met as a protectant; (a)pH=10; (b) pH=11; (c)pH=12; (d) pH=13; (e) copper powder particles size variation.

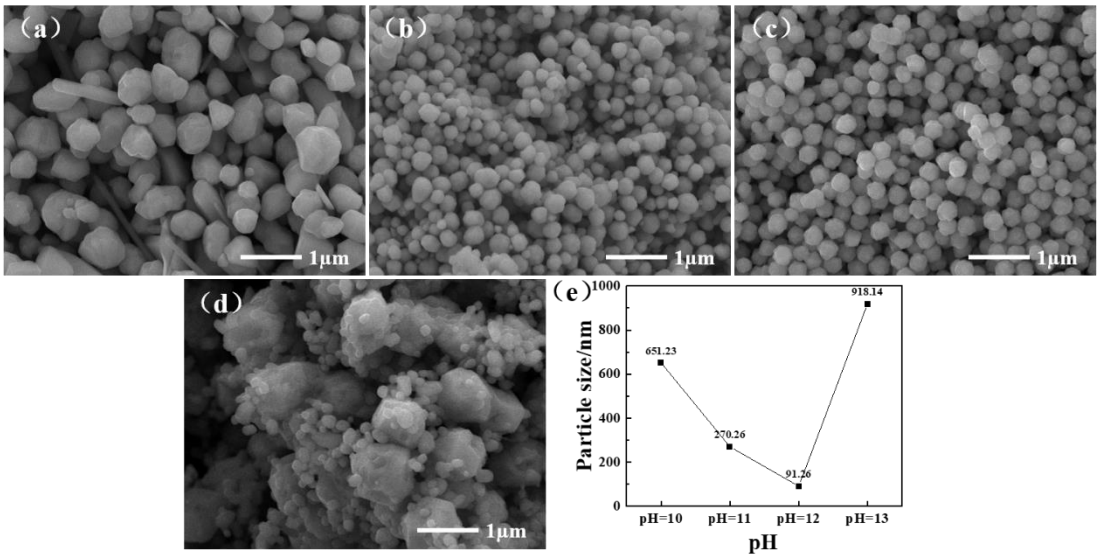

Fig. S2. SEM images and particle size variation of copper powder particles under different pH conditions using CTAB as a protectant; (a)pH=10; (b) pH=11; (c)pH=12; (d) pH=13; (e) copper powder particles size variation.

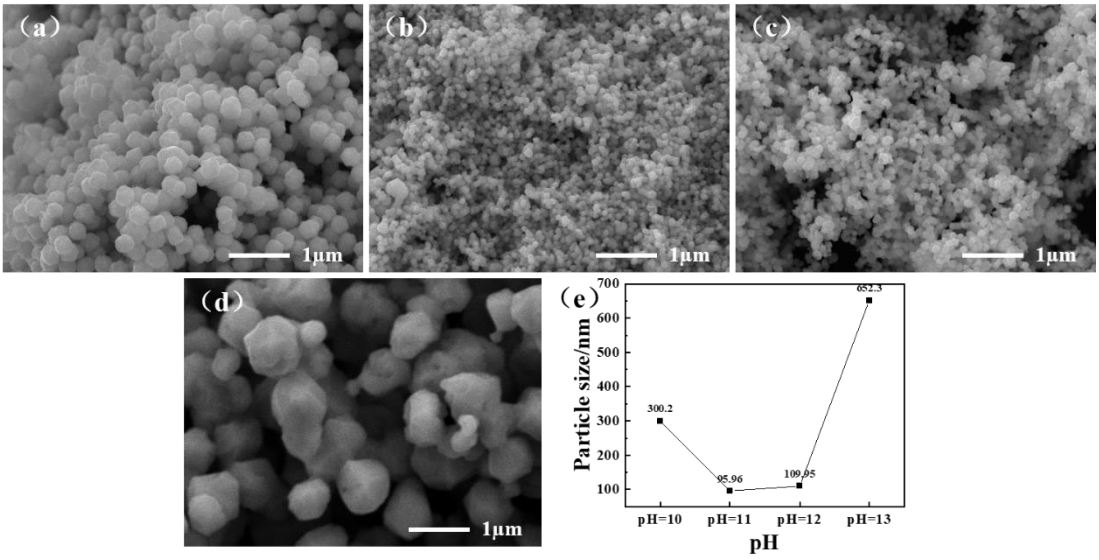

Fig. S3. SEM images and particle size variation of copper powder particles under different pH conditions using SSC as a protectant; (a)pH=10; (b) pH=11; (c)pH=12; (d) pH=13; (e) copper powder particles size variation.

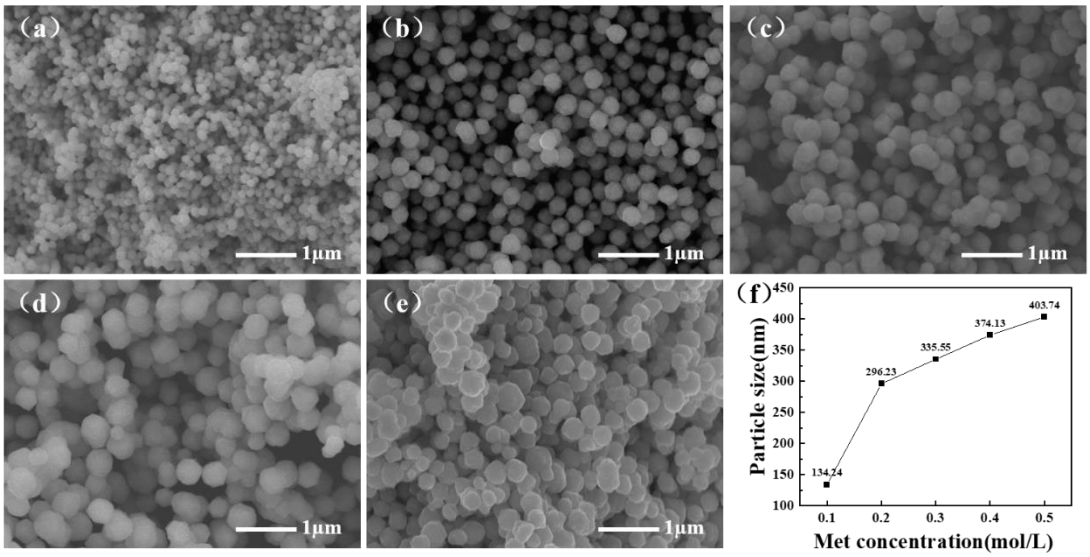

Fig. S4. SEM images and particle size variation of copper powder particles at different Met concentrations using Met as a protectant; (a)Met=0.1 mol/L; (b) Met=0.2 mol/L; (c) Met=0.3 mol/L; (d) Met=0.4 mol/L; (e) Met=0.5 mol/L; (f) copper powder particles size variation.

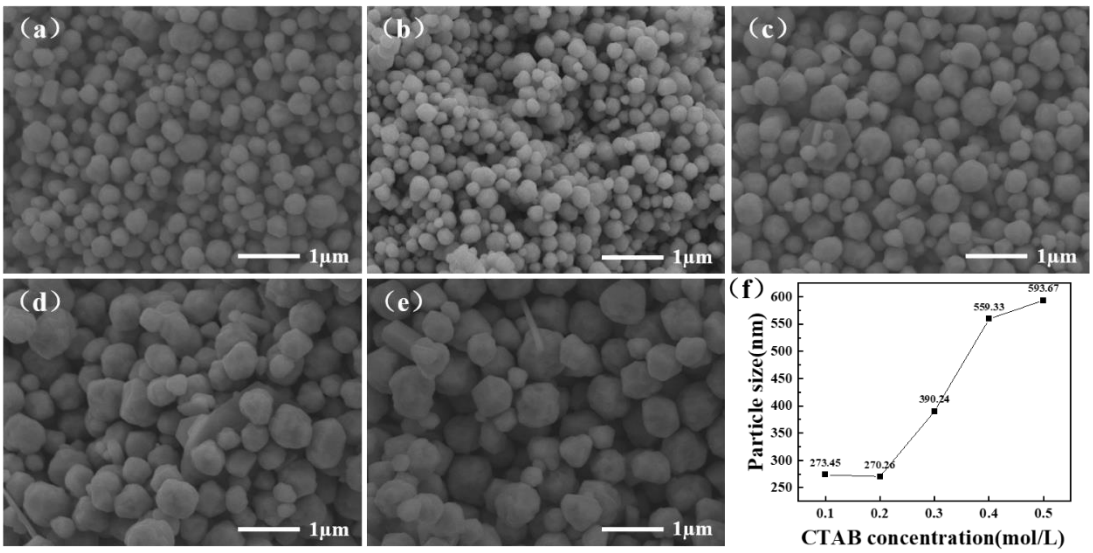

Fig. S5. SEM images and particle size variation of copper powder particles at different Met concentrations using CTAB as a protectant; (a)CTAB=0.1 mol/L; (b) CTAB=0.2 mol/L; (c) CTAB=0.3 mol/L; (d) CTAB=0.4 mol/L; (e) CTAB=0.5 mol/L; (f) copper powder particles size variation.

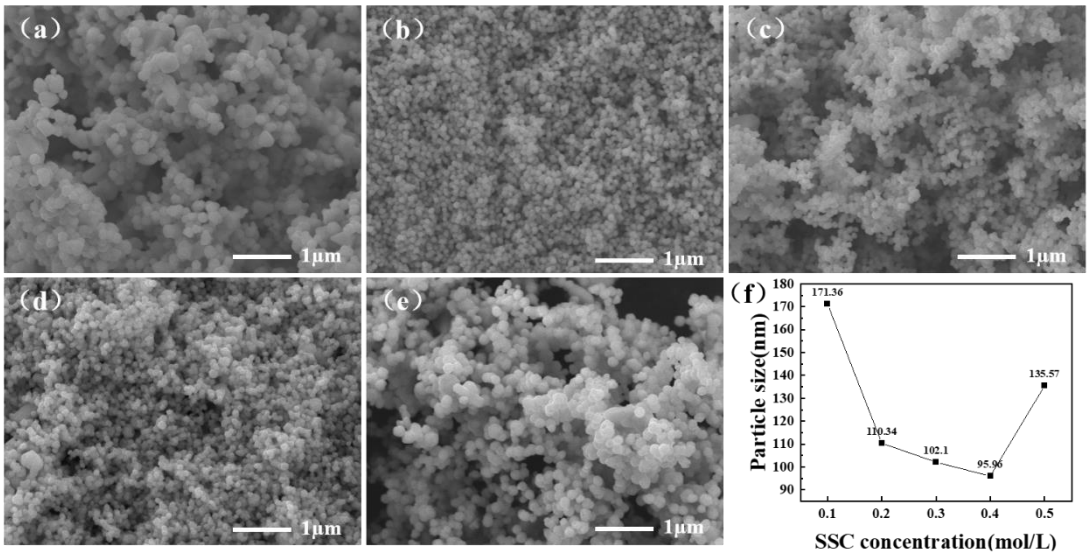

Fig. S6. SEM images and particle size variation of copper powder particles at different Met concentrations using SSC as a protectant; (a)SSC=0.1 mol/L; (b) SSC=0.2 mol/L; (c) SSC=0.3 mol/L; (d) SSC=0.4 mol/L; (e) SSC=0.5 mol/L; (f) copper powder particles size variation.

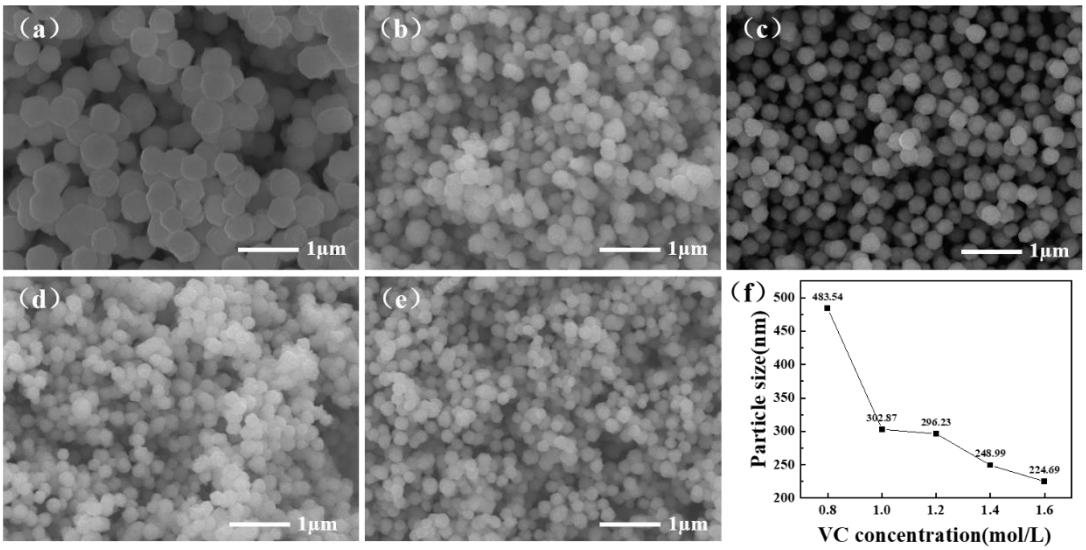

Fig. S7. SEM images and particle size variation of copper powder particles at different $C_6H_8O_6$ concentrations using Met as a protective agent; (a) $C_6H_8O_6$=0.8 mol/L; (b) $C_6H_8O_6$=1.0 mol/L; (c) $C_6H_8O_6$=1.2 mol/L; (d) $C_6H_8O_6$=1.4 mol/L; (e) $C_6H_8O_6$=1.6 mol/L; (f) copper powder particles size variation.

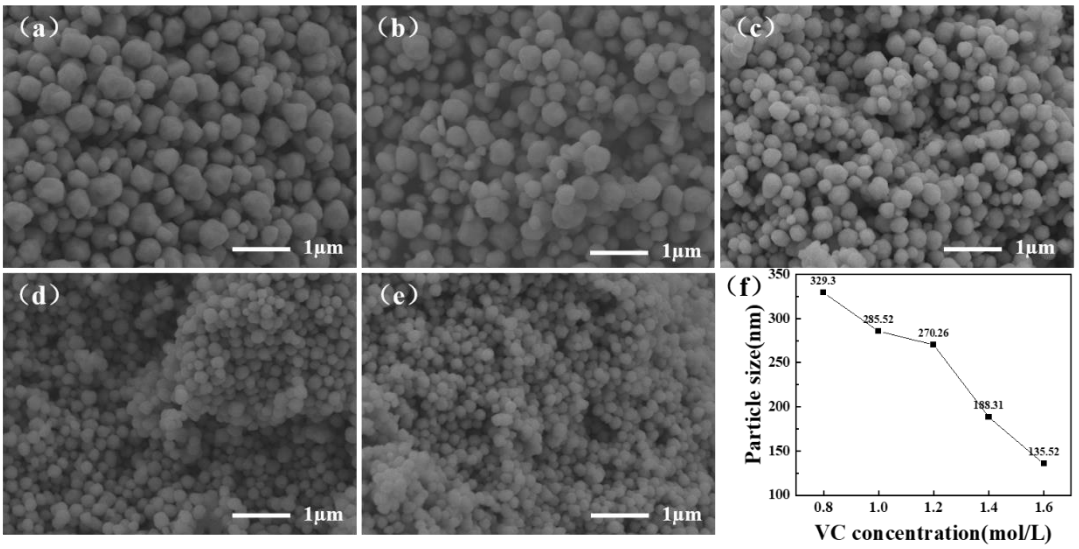

Fig. S8. SEM images and particle size variation of copper powder particles at different $C_6H_8O_6$ concentrations using CTAB as a protective agent; (a) $C_6H_8O_6$=0.8 mol/L; (b) $C_6H_8O_6$=1.0 mol/L; (c) $C_6H_8O_6$=1.2 mol/L; (d) $C_6H_8O_6$=1.4 mol/L; (e) $C_6H_8O_6$=1.6 mol/L; (f) copper powder particles size variation.

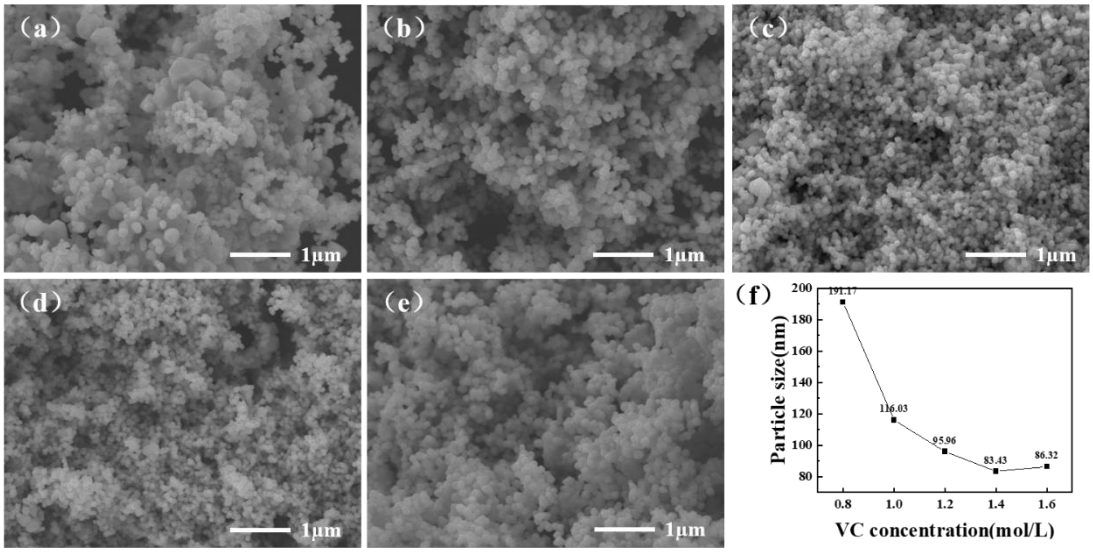

Fig. S9. SEM images and particle size variation of copper powder particles at different $C_6H_8O_6$ concentrations using SSC as a protective agent; (a) $C_6H_8O_6$=0.8 mol/L; (b) $C_6H_8O_6$=1.0 mol/L; (c) $C_6H_8O_6$=1.2 mol/L; (d) $C_6H_8O_6$=1.4 mol/L; (e) $C_6H_8O_6$=1.6 mol/L; (f) copper powder particles size variation.

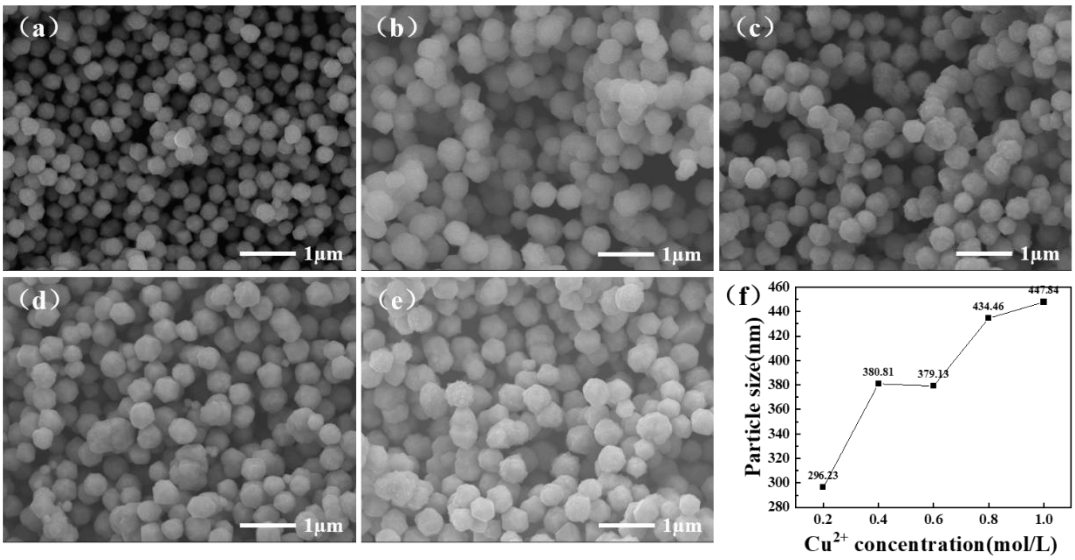

Fig. S10. SEM images and particle size variation of copper powder particles with different Cu^{2+} concentrations using Met as a protectant; (a) Cu^{2+}=0.2 mol/L; (b) Cu^{2+}=0.4 mol/L; (c) Cu^{2+}=0.6 mol/L; (d) Cu^{2+}=0.8 mol/L; (e) Cu^{2+}=1.0 mol/L; (f) copper powder particles size variation.

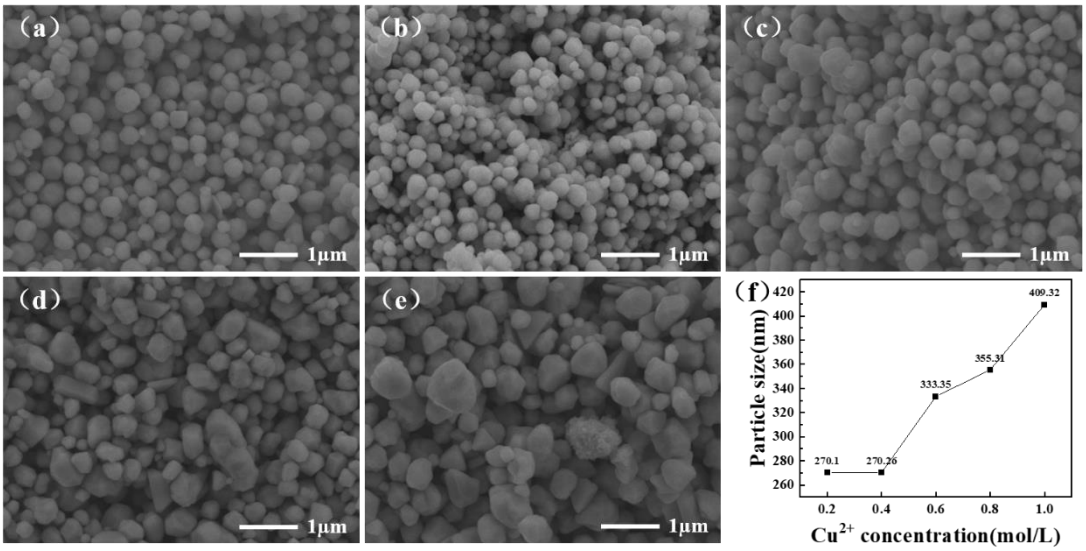

Fig. S11. SEM images and particle size variation of copper powder particles with different Cu^{2+} concentrations using CTAB as a protectant; (a) Cu^{2+}=0.2 mol/L; (b) Cu^{2+}=0.4 mol/L; (c) Cu^{2+}=0.6 mol/L; (d) Cu^{2+}=0.8 mol/L; (e) Cu^{2+}=1.0 mol/L; (f) copper powder particles size variation.

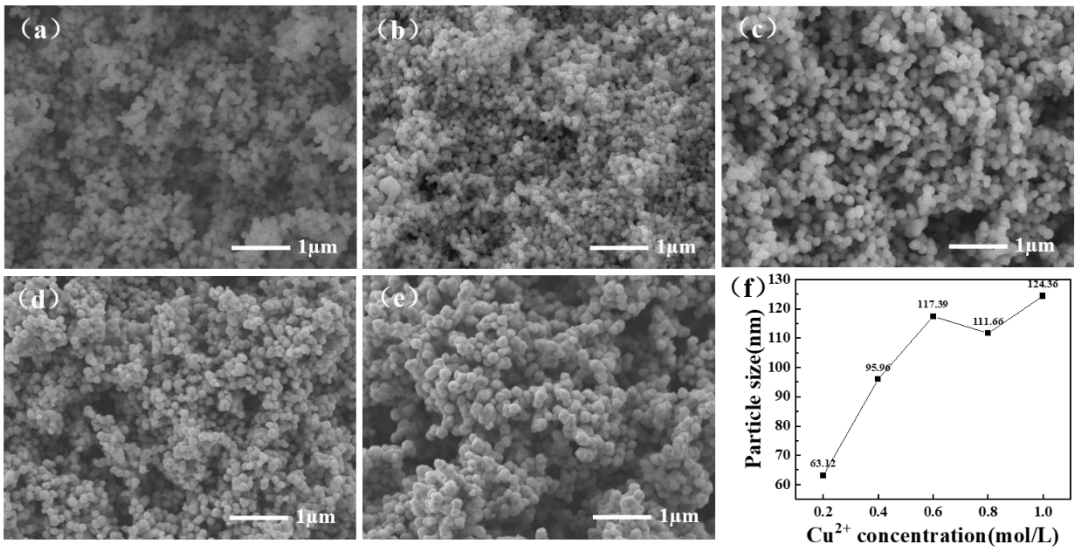

Fig. S12. SEM images and particle size variation of copper powder particles with different Cu^{2+} concentrations using SSC as a protectant; (a) Cu^{2+}=0.2 mol/L; (b) Cu^{2+}=0.4 mol/L; (c) Cu^{2+}=0.6 mol/L; (d) Cu^{2+}=0.8 mol/L; (e) Cu^{2+}=1.0 mol/L; (f) copper powder particles size variation.

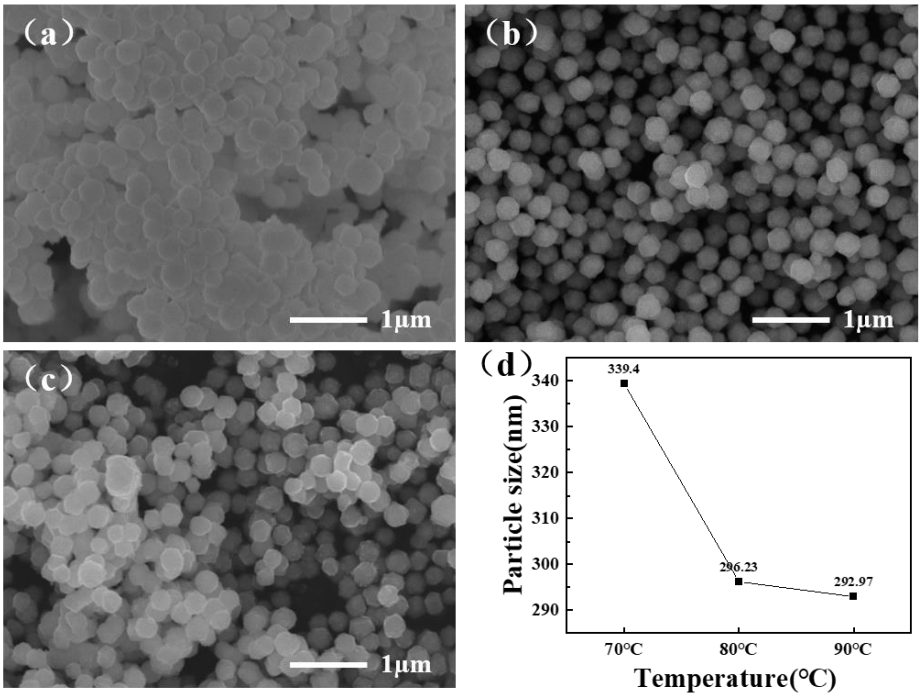

Fig. S13. SEM images and particle size variation of copper powder particles at different temperatures using Met as a protectant; (a) T=70℃; (b) T=80℃; (c) T=90℃; (d) copper powder particles size variation.

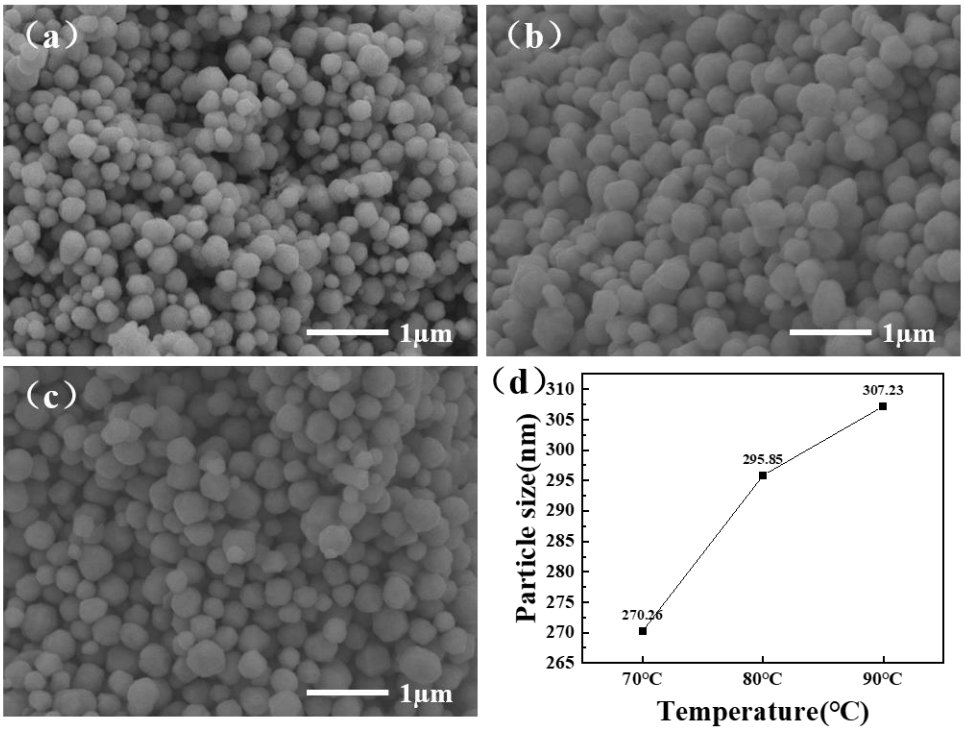

Fig. S14. SEM images and particle size variation of copper powder particles at different temperatures using CTAB as a protectant; (a) T=70℃; (b) T=80℃; (c) T=90℃; (d) copper powder particles size variation.

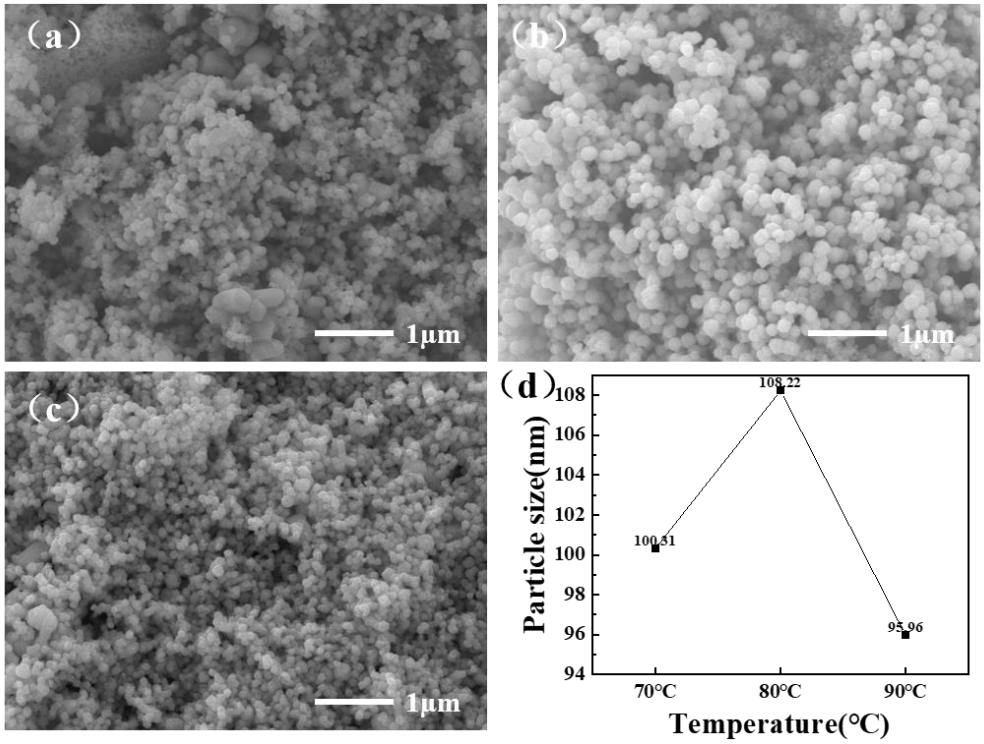

Fig. S15. SEM images and particle size variation of copper powder particles at different temperatures using SSC as a protectant; (a) T=70°C; (b) T=80°C; (c) T=90°C; (d) copper powder particles size variation.

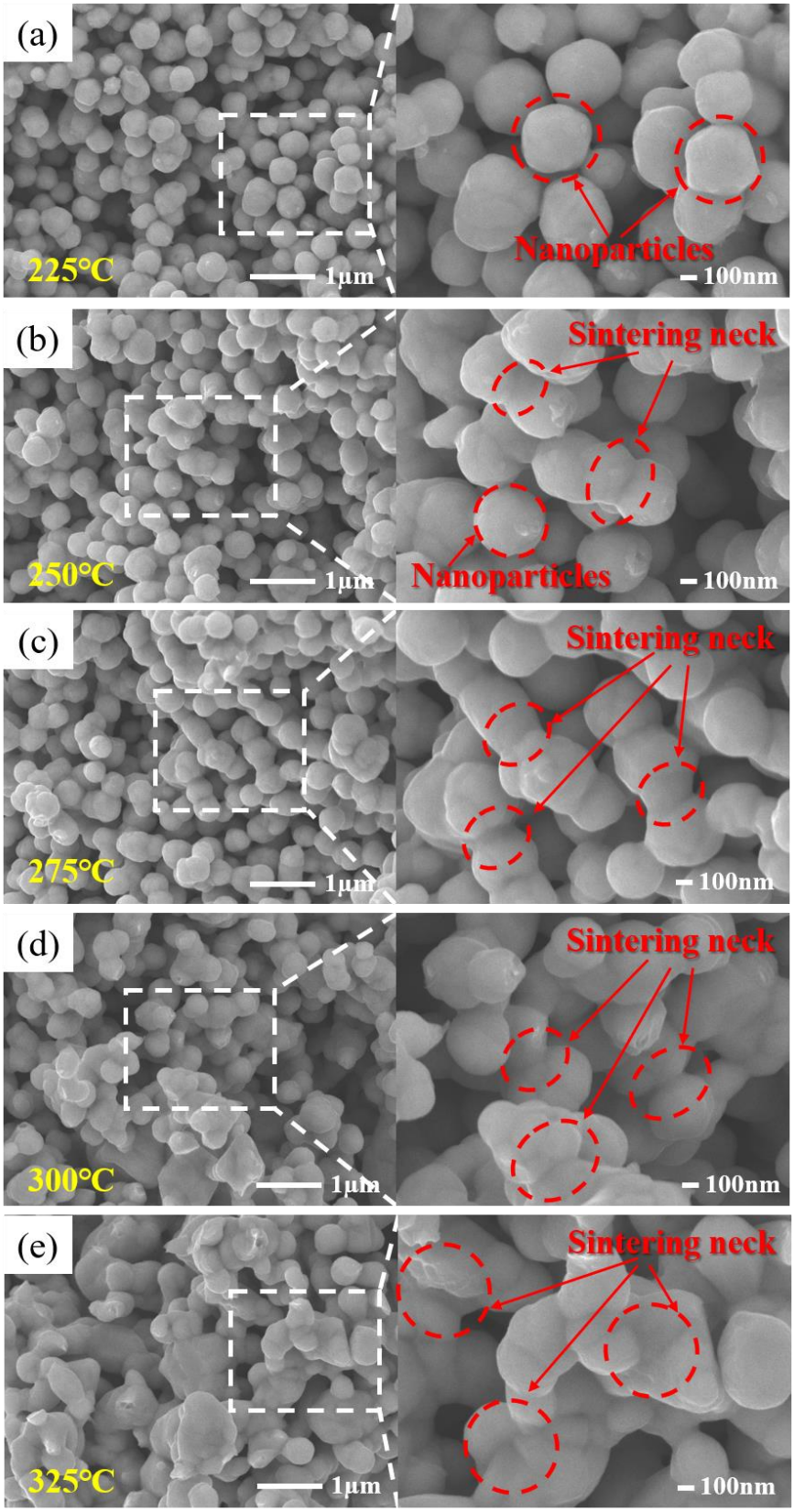

Fig. S16. SEM cross-sectional micrographs of copper nanoflakes held at different sintering temperatures for 30 min: (a) 225°C; (b) 250°C; (c) 275°C; (d) 300°C; (e) 325°C.